The International Journal of Advanced Manufacturing Technology (2019) 101:1227–1234
https://doi.org/10.1007/s00170-018-3004-8

ORIGINAL ARTICLE

Experimental study on the variance of mechanical properties of polyamide 6 during multi-layer sintering process in selective laser sintering

Zhicheng Ling[1] · Jinzhe Wu[1] · Xiang Wang[1] · Xiaofeng Li[1] · Jinjin Zheng[1]

Received: 14 May 2018 / Accepted: 6 November 2018 / Published online: 16 November 2018

Abstract
During the selective laser sintering layer-by-layer manufacturing process, many factors such as the ambient temperature and the densification effect will influence the mechanical properties of sintered specimens. In the experimental study, the porosity ratio, crystallinity, and tensile strength of sintered specimens with different ambient temperatures and layers were analyzed. The results indicated that when the ambient temperature rose from 25 to 180 °C, the average porosity ratio decreased from 60% at 25 °C to 39.7–38.7% at 140–180 °C; the relative crystallinity and tensile strength reached a maximum value of 34% and 10 MPa at 140 °C with the same number of sintered layers. According to the measurement of sintered specimens with different layers, the porosity ratio rapidly reduced by 21% from 3 to 10 layers, and the tensile strength improved by 22.5 MPa. When the number of sintered layers reached 10, the change of the porosity ratio and tensile strength were relatively slow, and it would almost disappear as the number of layers exceeded 14. The results showed that the densification process and energy accumulation effect were beneficial to reduce the porosity ratio of specimens, thereby improving its tensile strength in the early period of laser sintering.

Keywords Selective laser sintering · Layer-by-layer sintering · Tensile strength · Porosity ratio · Crystallinity

1 Introduction

Selective laser sintering (SLS) is one of the main processes in the additive manufacturing field. It applies laser beam as a heat source to sinter selectively powder materials layer by layer to obtain three-dimensional solid structures [1, 2]. Since the instantaneous high energy of laser can be used to sinter a variety of materials (metal powders, engineering plastic powders, etc.), this additive manufacturing technology has become the focus of many fields, such as industrial and medical applications. Accordingly, the mechanical properties of structures or parts that were manufactured by SLS technology are one of the important indexes for their practical applications. The effect of laser sintering process on the mechanical properties of sintered parts with different materials has been studied continuously by many scholars [3–5]. At present, there are many works on the optimization of laser sintering process parameters and mechanical properties of metal powders (stainless steel powders, titanium alloy powders, etc.) [6–8]. However, engineering plastics have become one of the most widely used materials in the industrial field due to its low density, high specific strength and strong corrosion resistance, etc. Therefore, the research on the SLS process and mechanical properties of engineering plastic powder has also drawn continuous concern [5, 9–12]. Typically, polyamide 6 (PA6), as one of the common engineering plastics, is widely used, because it not only has the advantages of engineering plastics, but also has high tensile strength. So, many

✉ Xiang Wang
wxyf@ustc.edu.cn

Zhicheng Ling
lingzhic@mail.ustc.edu.cn

Jinzhe Wu
jzw2014@mail.ustc.edu.cn

Xiaofeng Li
lxf@ustc.edu.cn

Jinjin Zheng
jjzheng@ustc.edu.cn

[1] Department of Precision Mechanic and Precision Instrumentation, University of Science and Technology of China, Hefei 230027, People's Republic of China

scholars have developed the research on the SLS sintering process and the mechanical properties of the sintered parts of PA6 powder. For example, Salmoria et al. investigated the tensile strength of sintered specimens of PA6 and PA12 mixed powder [13]. Zarringhalam et al. [14, 15] studied the mechanical properties of PA12 powder by observing the powder melting behavior and the microstructure during the SLS sintering process.

During the complex process of melting and cooling, there are many influencing factors. Parameters such as laser power and scanning speed have an effect on the sintering process; furthermore, the ambient temperature (preheating and holding temperature) of the sintering process has an impact on the crystallization state and the porosity ratio of sintered specimens. Meanwhile, the flow of the melt in the upper and lower layers will reduce the porosity ratio of the specimens. At the same time, the energy accumulation effect of the sintered powder bed will also influence the sintering process.

Therefore, in this article, according to this layer-by-layer additive manufacturing feature of SLS, the tensile strength of sintered specimens was used as an evaluation indicator. The process parameters were optimized by experimental analysis. The tensile strength of sintered specimens with different layers was measured to understand the variance of tensile strength of sintered specimens during the process of layer-by-layer sintering. It will provide a fundamental basis for the improvement of the quality of SLS structural parts of engineering plastic powder material.

2 Experimental design

The SLS process (Fig. 1) makes 3D objects built by selectively fusing together successive layers of powdered material. The laser beam moves with a certain scanning speed and track to obtain a sintering line that is adapted to the width of the molten pool. The laser beam scans line by line with a suitable scanning space l to achieve an effective melting between lines. By this way, multiple lines are melted and solidified to form a thin plane. At the same time, the laser energy applied to the lower layer (solidified layer) through the thickness h of the powder layer makes two layers melted together partially. Finally, the three-dimensional structure is manufactured by SLS.

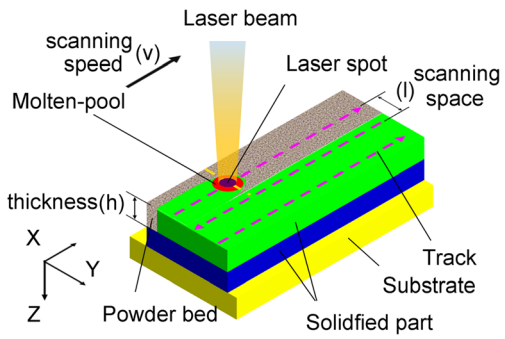

Fig. 1 Schematic diagram of the SLS process

Therefore, the parameters of the SLS process for engineering plastic powder are the laser wavelength λ, laser power P, laser spot diameter d, scanning speed v, scanning space l, and layer thickness h. Since the PA6 material studied in this experiment is a kind of semi-crystalline polymer, the ambient temperature of the sintering process has a direct impact on its crystallinity, so the ambient temperature T_0 is also one of the main parameters.

The engineering plastic powder for this experiment is pure polyamide 6 with particle size ranging from 90 to 106 μm (the average particle size $d_0 = 0.1$ mm). The density of the material is 1.13 g/cm^3 by ISO 1183-1:2012; the melting point is 220 °C by ISO 3416:2000. The heat source is a 0–30-W CO_2 laser ($\lambda = 10.6$ μm) with a spot size of 0.24 mm. The maximum scanning speed v_{max} is 3000 mm/s.

In general, tensile strength is the most basic and important strength index, which is not only an important basis for engineering design, material evaluation, and process optimization, but also the basic data for predicting other mechanical properties of materials (fatigue strength, fracture properties, etc.). Therefore, in this paper, the mechanical properties of sintered specimens were measured to understand the variance of tensile strength of sintered specimens during the process of layer-by-layer sintering. The tensile specimens used in this research were rectangle specimens 65 mm × 10 mm by ISO 527-2:1993 (gauge length 50 mm).

3 Experiments, results, and discussion

3.1 Effect of ambient temperature on tensile strength

3.1.1 Experiment and the measurement of tensile strength

It is necessary to select the parameters in the SLS process. The laser spot diameter used in this experiment was 0.24 mm. If the scanning space is too large, the lines cannot be sintered effectively. However, if the scanning space is too small, it may cause overburning in the overlapping area. According to the previous study [16], the scanning method was S-type, and the appropriate scanning space l was 0.3 mm. And the average particle diameter d_0 was 0.1 mm, in order to achieve the effective fusion of the upper and lower layers; the effective minimum layer thickness h was 0.1 mm.

During the laser sintering process, the injection energy is mainly affected by both the laser powder P and the scanning speed v. Actually, when the laser energy is too small, the powder cannot be effectively sintered and will be difficult to form, whereas too large laser energy causes the high temperature of local molten pool. When the temperature exceeds the thermal decomposition temperature of material, it will cause

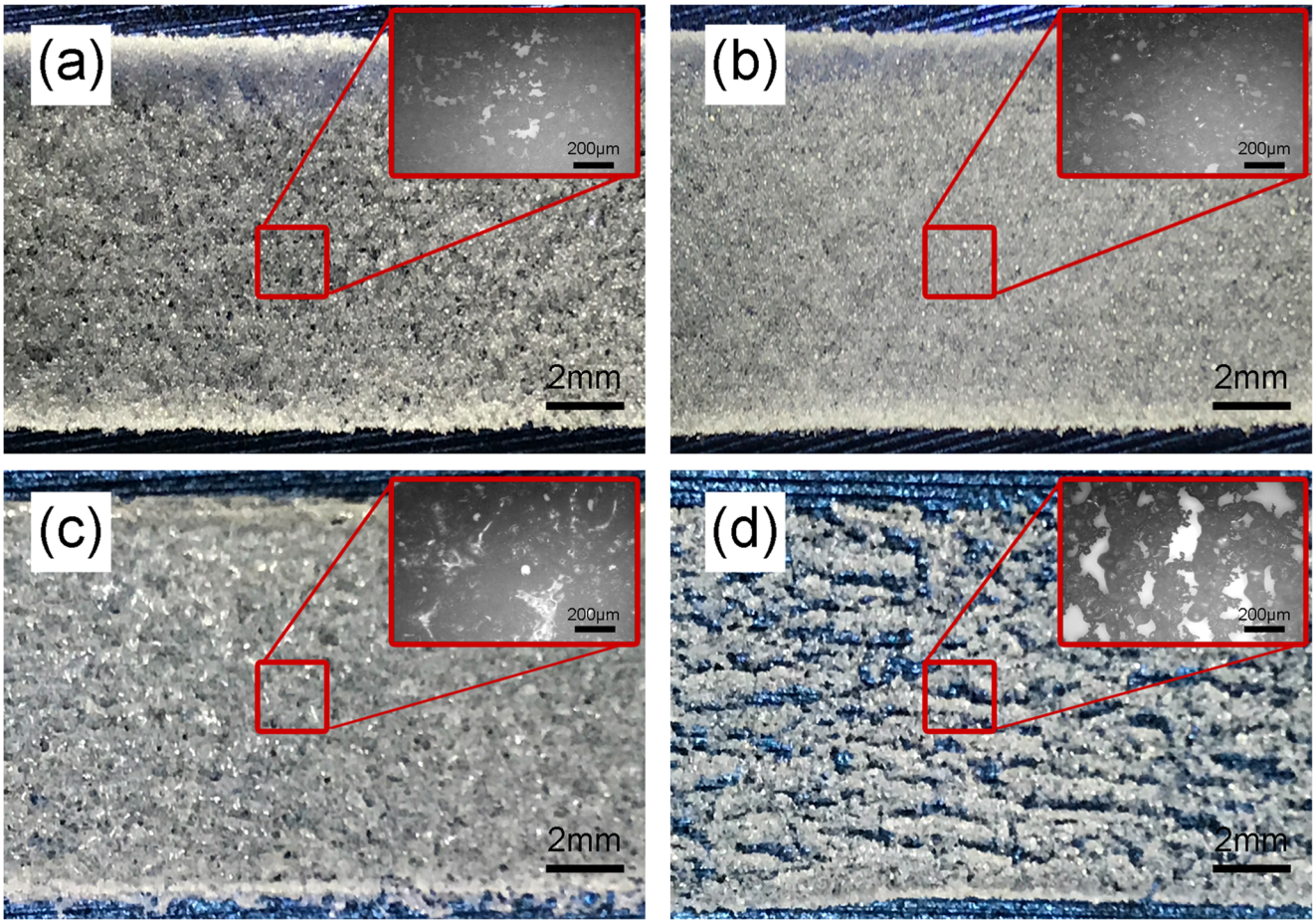

Fig. 2 Photographs and OM micrographs (local enlarged images) of the surface of PA6 specimens produced by different processing parameters (T_0 = 25 °C). **a** P = 5 W, v = 400 mm/s. **b** P = 7 W, v = 400 mm/s. **c** P = 7 W, v = 300 mm/s. **d** P = 7 W, v = 200 mm/s

overburning and thermal decomposition of the powder. This paper used the orthogonal test to find the appropriate laser power P and laser scanning speed v. The experiment was studied by the orthogonal test with two factors and five levels [17, 18]. The range of laser power and scanning speed were chosen based on the previous study [14]. The values of P were 3, 5, 7, 9, and 11 W. The values of v were 100, 200, 300, 400, and 500 mm/s. The number of sintered layers was 4. The ambient temperature T_0 was 25 °C.

According to the orthogonal experiment table, the sintering experiment was carried out.

The experiment result showed that when the laser power P was 3 W or the scanning speed v was 500 mm/s, sintered samples all had lots of powders that were not sintered effectively and could not be formed. When P was 11 W or v was 100 mm/s, there was an overburnt phenomenon during sintering. Although it can be sintered more effectively at 5 W 200 mm/s, there still exist some apparent pores. When

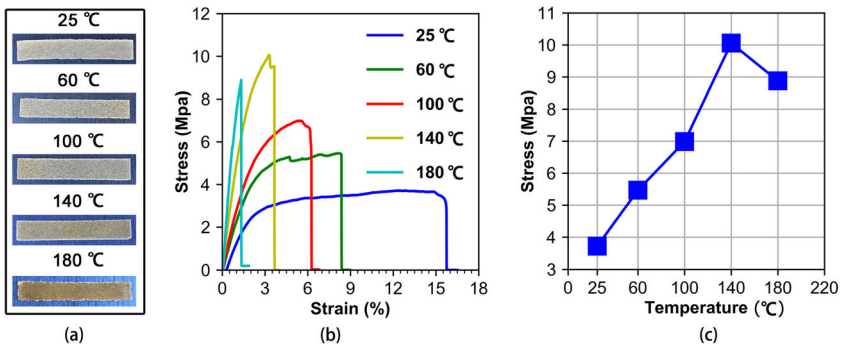

Fig. 3 **a** Photographs showing the surface of PA6 specimens under different T_0. **b** Stress-strain curve of sintered specimens under different T_0. **c** Average tensile strength under different T_0

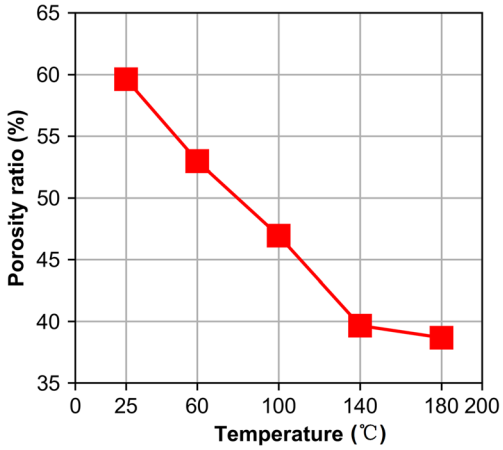

Fig. 4 Average porosity ratio under different T_0

laser power was 9 W, the speed range was 200~400 mm/s; although the overburnt phenomenon was not as serious as that at 11 W, the specimen still cannot be formed effectively.

Partial experimental results are shown in Fig. 2. Figure 2a is the sintered specimen with $P = 5$ W, $v = 400$ mm/s. When sintering at a low laser power, PA6 powder cannot be sintered effectively, so there are many unmelted particles and holes on the surface. When the sintering energy increases, the laser power $P = 7$ W, the scanning speed $v = 400$ mm/s, the sintering result is better, and the unmelted particles are fewer, and the surface of the sintered specimen is more compact as Fig. 2b shows.

Figure 2c shows that if the sintering energy further increases, when $P = 7$ W and $v = 300$ mm/s, the sintered specimen is slightly overburnt due to the large energy. Subsequently, when the laser power P is 7 W and the scanning speed v is 200 mm/s, the sintered specimen is overburnt seriously, as Fig. 2d shows.

Although, we can get better-sintered specimens (7 W, 400 mm/s) at 25 °C, as Fig. 2b shows. However, due to the fast cooling speed at 25 °C, the temperature field is not uniform and there will be a large residual stress. Larger residual stresses will deform the sintered specimen [19, 20]. Therefore, it is difficult to perform multi-layer sintering at 25 °C; furthermore, the maximum number of sintered layers at this ambient temperature is 4. Preheating and heat preservation are beneficial to the uniformity of the temperature field and help to slow down the cooling rate of the molten pool. Therefore, this article selects different ambient temperatures (preheating and holding temperature) T_0 (25, 60, 100, 140, and 180 °C) for further experiments in order to understand the effect of ambient temperature on the tensile strength.

The sintered specimens under different T_0 are shown in Fig. 3a. The number of layers is 4 and the average thickness H is 0.38 mm. Tensile strength of the sintered specimens tested by Electromechanical Universal Testing Machine (MTS Systems (China) Co., Ltd.) with different T_0 is shown in Fig. 3b and Fig. 3c. Figure 3c is the average tensile strength σ_{max} of the sintered specimens under different T_0. The result shows that the tensile strength is 3.7 MPa at 25 °C. The tensile strength increases as the ambient temperature rises, and reaches a maximum value of 10 MPa at 140 °C. The tensile strength decreases to 8.9 MPa at 180 °C.

During sintering, the effective melting of particles and the flow of the molten pool will impact the void space between powder particles. With the increase of the ambient temperature, the powder particles can be melted effectively; furthermore, the cooling rate of the molten pool becomes slower and the flowing time of the molten material becomes longer, which will facilitate the filling of the holes. Therefore, proper preheating and insulation will help reduce the holes inside of the samples, and then increase its tensile strength.

On the other hand, PA6 is a typical semi-crystalline polymer; the ambient temperature will have a significant influence on the crystalline state of specimens during the condensation process [21–23]. And the degree of crystallization of semi-crystalline polymers will have an impact on their mechanical properties [24]. So, this paper measured the porosity ratio and crystallinity of sintered specimens at different ambient temperatures to understand the influence of ambient temperature on the porosity ratio, crystallinity, and tensile strength.

3.1.2 Measurement of porosity ratio

The porosity ratio of sintered specimens is measured by the density method which can be described as $P_0\ (\%) = (1 - \rho_m/\rho_0) \times 100\%$ (ρ_m is the density of the sintered sample, ρ_0 is the theoretical density of PA6) [25]. The average porosity ratio P_0 at different T_0 is shown in Fig. 4. The porosity ratio P_0 is 60% at 25 °C. It decreases as the ambient temperature rises. When T_0 is 140 °C, P_0 rapidly decreases to 39.7%. When T_0 rises from 140 to 180 °C, the porosity ratio decreases by only 1%.

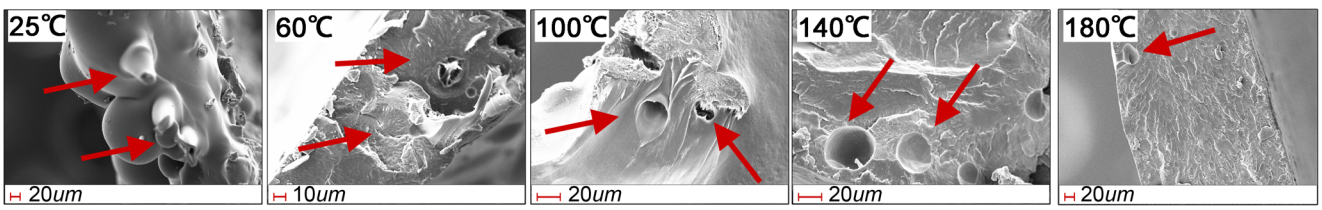

Fig. 5 SEM photomicrographs of the cross-sections of sintered specimens at different T_0

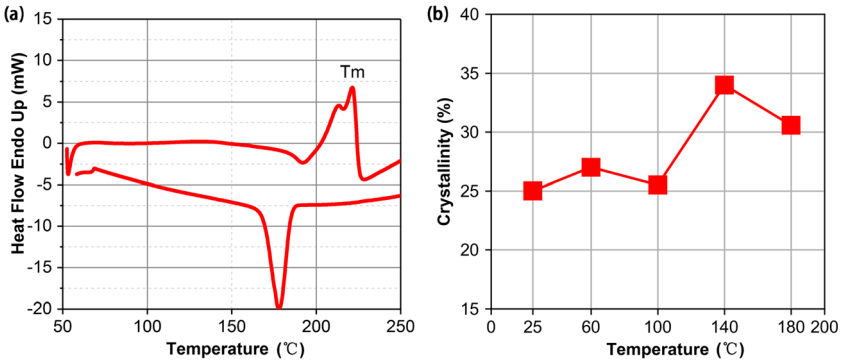

Fig. 6 **a** DSC curve of specimen at 140 °C. **b** The average crystallinity of specimens under different T_0

The SEM photomicrographs (ZEISS EVO 18) of the cross-sections of sintered specimens under different T_0 are shown in Fig. 5. The results show that the powder particles are fewer molten together at 25 °C. The particles are more molten together with T_0 increasing, but the specimens still have lots of holes at 100 °C. When T_0 is 140 °C, the cross-section of sintered specimen is denser, but still has some holes. The holes are fewer and the cross-section is nearly full when T_0 reaches 180 °C. Therefore, with the ambient temperature increasing, the porosity ratio of sintered specimen decreases gradually, and the process of laser sintering changes from the "SLS" process to "SLM" process. Fewer holes (lower porosity ratio) contribute to the continuity of the parts. As a result, lower porosity ratio can reduce stress centralizing during loading, preventing the crack initiation and propagation, increasing tensile strength.

3.1.3 Measurement of crystallinity

The different ambient temperatures T_0 will affect the cooling speed and crystallinity of specimens; hence, in order to understand the influence of T_0 on the crystallinity of the sintered specimens, this experiment measures the crystallinity of sintered specimens under different T_0 by using Diamond DSC (Shelton, CT 06484 USA). The DSC curve of specimen at 140 °C is shown in Fig. 6a. The crystallinity of sintered specimens can be calculated as $X_c\ (\%) = (\Delta H_m/\Delta H_{m100}) \times 100\%$, where ΔH_m is the melting enthalpy of the specimens and ΔH_{m100} (185.8 J/g) is the perfect crystals of polyamide 6 [26]. The average crystallinity under different T_0 is described in Fig. 6b. As the results shows, when $T_0 < 100$ °C, the average crystallinity X_c is about 25%. When $T_0 = 140$ °C, X_c increases to 34% with T_0 increasing. However, when X_c is over 140 °C, the crystallinity begins to decline and the crystallinity is 30% at 180 °C.

It can be seen that the increase of T_0 slows down the cooling rate of the molten pool during the laser sintering process, which contributes to the crystallinity of the sintered specimens. Higher crystallinity can increase the tensile strength of the parts. However, with T_0 increasing, the continuous injection of laser energy causes the overburnt phenomenon during multi-layer sintering (the sintered specimen at 180 °C is shown in Fig. 3a). Therefore, although the average porosity ratio of specimens is slightly lower at 180 °C (SEM image in Fig. 5 and the 38% porosity ratio at 180 °C in Fig. 6), the overburnt phenomenon might impact the crystallinity of the specimens, and the crystal microstructures. Furthermore, it will result in lower tensile strength. So, in this experiment, when the ambient temperature is 140 °C, the sintered specimens exhibit better sintering quality and tensile strength.

3.2 Effect of layer-by-layer sintering process on tensile strength

According to the previous experimental results, the multi-layer sintering experiment parameters were $P = 7$ W, $v = 400$ mm/s, $l = 0.3$ mm, $h = 0.1$ mm, and $T_0 = 140$ °C. The numbers of sintered layers N were 2, 3, 4, 6, 8, 10, 12, 14, 16, and 20. When $N < 3$, the quality of sintered specimens was poor and the specimens were fragile. So, this paper tested the tensile strength of sintered specimens no less than two layers.

The average tensile strength of sintered specimens with different N is shown in Fig. 6. At the beginning of SLS, the tensile strength rockets quickly, then it slowly increases from 27.6 to 30 MPa as N rising from 10 to 14. However, when $N >$

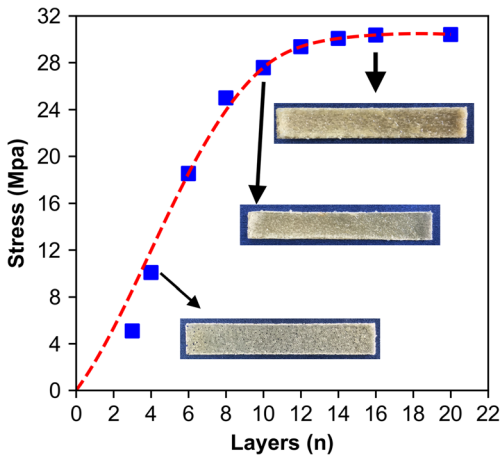

Fig. 7 Average tensile strength with different N

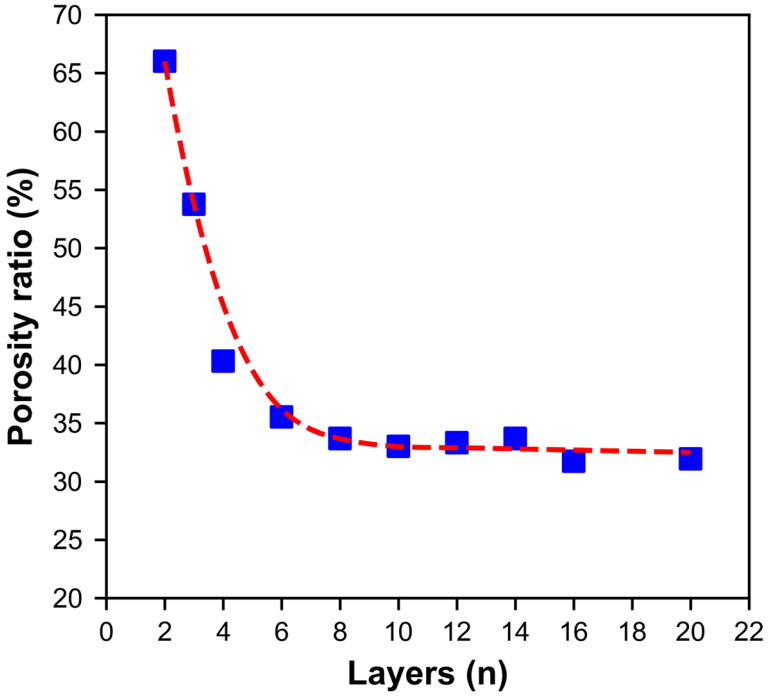

(a)

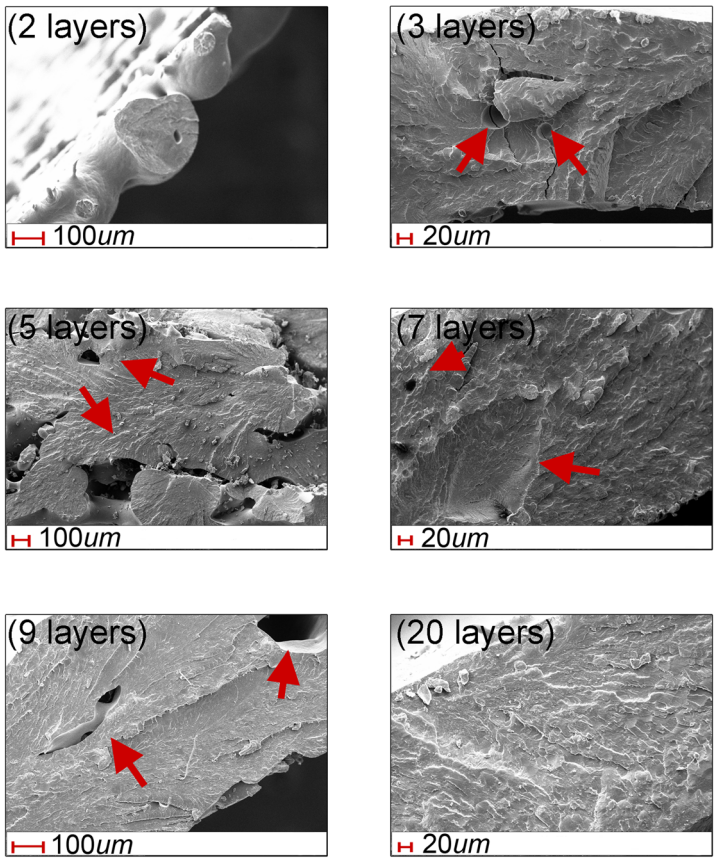

(b)

Fig. 8 **a** Average porosity ratio with different *N*. **b** SEM photomicrographs of the cross-sections of sintered specimens with different *N*

14, the tensile strength is nearly unchanged with N going up. The maximum tensile strength is 30.41 MPa when N is 20.

At the beginning of the layer-by-layer sintering process of the selective laser sintering, the amount of powder is little, and the volume of the molten pool is small. So, the ability of molten pool to fill the holes between the upper and lower layers is limited. However, the newly added powder particles are melted to form the new molten pool with N increasing, and the molten pool can fill up some of the holes on the surface of the previous sintered layer. Furthermore, the layer-by-layer sintering process will make a part of the solidified part melted again. The secondary flow of molten pool is even possible to fill some internal holes, which reduce the porosity ratio. Lower porosity ratio will increase the tensile strength.

The average porosity ratio and SEM photomicrographs of cross-sections of sintered specimens are shown in Fig. 8. According to the average porosity ratio with different N shown in Fig. 8a, at the beginning of sintering process, P_0 decreases from 54 to 33% quickly with N increasing from 3 to 10. However, when $N > 10$, the decrease of P_0 is slow. Furthermore, after N reaches 12, P_0 maintains in 32%. At the same time, during the layer-by-layer sintering process, the continuous injection of laser energy causes the energy accumulation effect. The actual temperature of powder particles and the ambient temperature will be increased accordingly. This effect is beneficial to slow down the cooling rate of the molten pool; furthermore, it will reduce the porosity ratio in the early stage of sintering when N is less. But, the effect of energy accumulation on reducing the porosity ratio will be weakened with N increasing. As a result, this effect will rise the temperature of powder bed, and then increase the risk of overburning (as Fig. 7 shows that the color of specimens' surface turns yellow).

According to Fig. 8b, the SEM photomicrographs of the cross-sections of sintered specimens show that there are larger holes on the fracture surface when N is 3. However, the sintered specimens undergo a rapid densification process with N increasing from 3 to 10. During this process, P_0 decreases rapidly and tensile strength increases fast. Furthermore, when $N > 10$, the densification process ends gradually, and the cross-sections of specimens are denser. So, the change of P_0 is relatively flat, and the tensile strength increases slowly after 10 layers. When the sintered specimens reach 20 layers, there are fewer holes on the cross-section of the specimen, which indicates that the sintering process has been transformed into a SLM process and the tensile strength has basically reached the relative maximum value.

4 Conclusion

In this paper, the optimized process parameters were obtained based on the orthogonal experiment ($P = 7$ W, $v = 400$ mm/s, $l = 0.3$ mm, $h = 0.1$ mm). The density method and SEM of specimens were used to measure and observe the holes in the sintered specimens. The crystallinity of sintered specimens with different ambient temperatures was measured by DSC. The effect of ambient temperature and process of layer-upon-layer sintering on the tensile strength of specimens were analyzed. The main conclusions are:

1. With the ambient temperature increasing, it can slow down the cooling rate of the sintered specimen which is beneficial to the flow of the molten pool; furthermore, it will reduce the porosity ratio of specimens and improve the crystallinity of specimens. According to the experimental results, with the ambient temperature increasing from 25 to 140 °C, the porosity ratio decreases by 20.3%, the crystallinity increases by 9%, and the tensile strength improves by 6.3 MPa. The crystallinity and tensile strength reach the highest when the ambient temperature is 140 °C.
2. There is a densification process during the sintering process. Firstly, when the number of layers is less than 10, with the number of layers increasing from 3 to 10, the porosity ratio decreases from 54 to 33% rapidly; furthermore, the tensile strength increases by 22.5 MPa. Secondly, with the number of layers increasing, the effect of densification process begins to weaken. The tensile strength increases by 2.4 MPa. Finally, with the densification process ending, the porosity ratio decreases by only 2% from 14 layers to 20 layers. The tensile strength increases by only 0.41 MPa.
3. During the process of layer-upon-layer sintering, the energy accumulation effect will be beneficial to the flow of molten pool and reduce the porosity ratio in the early stage. But excessive energy accumulation will cause the overburnt phenomenon, and then will make the specimens' surface turn yellow.

This paper provides a foundation for the application of SLS structures of engineering plastic powder materials. However, the experiment shows that energy accumulation effect will also influence the sintering process; so, a further study for improving the mechanical properties of sintered specimens through the method of transient process parameters will be investigated.

Acknowledgements The technical assistance from State Key Laboratory (USTC) is gratefully acknowledged.

Funding information This study received financial support from the Key Research and Development Program of Anhui (grant number 1704a0902051).

References

1. Jacobs PF (1992) Rapid prototyping & manufacturing: fundamentals of stereolithography. Society of Manufacturing Engineers
2. Bourell DL, Marcus HL, Barlow JW, Beaman JJ (1992) Selective laser sintering of metals and ceramics. Int J Powder Metall 28(4): 369–381
3. Eshraghi S, Das S (2010) Mechanical and microstructural properties of polycaprolactone scaffolds with one-dimensional, two-dimensional, and three-dimensional orthogonally oriented porous architectures produced by selective laser sintering. Acta Biomater 6(7):2467–2476. https://doi.org/10.1016/j.actbio.2010.02.002
4. Chacón JM, Caminero MA, García-Plaza E, Núñez PJ (2017) Additive manufacturing of PLA structures using fused deposition modelling: effect of process parameters on mechanical properties and their optimal selection. Mater Des 124:143–157. https://doi.org/10.1016/j.matdes.2017.03.065
5. Mägi P, Krumme A, Pohlak M (2016) Recycling of PA-12 in additive manufacturing and the improvement of its mechanical properties. Key Eng Mater 674:9–14. https://doi.org/10.4028/www.scientific.net/KEM.674.9
6. Karimi P, Raza T, Andersson J, Svensson LE (2017) Influence of laser exposure time and point distance on 75-μm-thick layer of selective laser melted alloy 718. Int J Adv Manuf Technol 94(5–8):2199–2207. https://doi.org/10.1007/s00170-017-1019-1
7. Feng Q, Tang Q, Liu Y, Setchi R, Soe S, Ma S, Bai L (2017) Quasi-static analysis of mechanical properties of Ti6Al4V lattice structures manufactured using selective laser melting. Int J Adv Manuf Technol 94(5–8):2301–2313. https://doi.org/10.1007/s00170-017-0932-7
8. Fayed EM, Elmesalamy AS, Sobih M, Elshaer Y (2017) Characterization of direct selective laser sintering of alumina. Int J Adv Manuf Technol 94(5–8):2333–2341. https://doi.org/10.1007/s00170-017-0981-y
9. Zhu W, Yan C, Shi Y, Wen S, Liu J, Shi Y (2015) Investigation into mechanical and microstructural properties of polypropylene manufactured by selective laser sintering in comparison with injection molding counterparts. Mater Des 82:37–45. https://doi.org/10.1016/j.matdes.2015.05.043
10. Lisi Leite J, Salmoria GV, Paggi RA, Ahrens CH, Pouzada AS (2011) Microstructural characterization and mechanical properties of functionally graded PA12/HDPE parts by selective laser sintering. Int J Adv Manuf Technol 59(5–8):583–591. https://doi.org/10.1007/s00170-011-3538-5
11. Salmoria GV, Ahrens CH, Klauss P, Paggi RA, Oliveira RG, Lago A (2007) Rapid manufacturing of polyethylene parts with controlled pore size gradients using selective laser sintering. Mater Res 10(2):211–214
12. Kim J, Creasy TS (2004) Selective laser sintering characteristics of nylon 6/clay-reinforced nanocomposite. Polym Test 23(6):629–636. https://doi.org/10.1016/j.polymertesting.2004.01.014
13. Salmoria GV, Leite JL, Vieira LF, Pires ATN, Roesler CRM (2012) Mechanical properties of PA6/PA12 blend specimens prepared by selective laser sintering. Polym Test 31(3):411–416. https://doi.org/10.1016/j.polymertesting.2011.12.006
14. Zarringhalam H, Majewski C, Hopkinson N (2009) Degree of particle melt in nylon-12 selective laser-sintered parts. Rapid Prototyp J 15(2):126–132. https://doi.org/10.1108/13552540910943423
15. Zarringhalam H, Hopkinson N, Kamperman NF, de Vlieger JJ (2006) Effects of processing on microstructure and properties of SLS nylon 12. Mater Sci Eng A 435-436:172–180. https://doi.org/10.1016/j.msea.2006.07.084
16. Zhou W, Wang X, Hu J, Zhu X (2013) Melting process and mechanics on laser sintering of single layer polyamide 6 powder. Int J Adv Manuf Technol 69(1–4):901–908. https://doi.org/10.1007/s00170-013-5113-8
17. Cavazzuti M (2013) Design of experiments. In: Optimization methods. Springer, pp 13–42
18. Wu H (2013) Application of orthogonal experimental design for the automatic software testing. In: Appl Mech Mater. Trans Tech Publ, pp 812–818
19. Ren JW, Dong LJ (2012) Effect of process parameters on residual thermal stress in laser sintering process. Innovation and Sustainability of Modern Railway 551–556
20. Mercelis P, Kruth JP (2006) Residual stresses in selective laser sintering and selective laser melting. Rapid Prototyp J 12(5):254–265. https://doi.org/10.1108/13552540610707013
21. Fischer C, Seefried A, Drummer D (2017) Crystallization and component properties of polyamide 12 at processing-relevant cooling conditions. Polym Eng Sci 57(4):450–457. https://doi.org/10.1002/pen.24441
22. Zhang X, Yang G, Lin J (2006) Crystallization behavior of nylon 11/montmorillonite nanocomposites under annealing. J Appl Polym Sci 102(6):5483–5489. https://doi.org/10.1002/app.23900
23. Dadbakhsh S, Verbelen L, Verkinderen O, Strobbe D, Van Puyvelde P, Kruth J-P (2017) Effect of PA12 powder reuse on coalescence behaviour and microstructure of SLS parts. Eur Polym J 92:250–262. https://doi.org/10.1016/j.eurpolymj.2017.05.014
24. Zhang X, Li YB, Zuo Y, Lv GY, Mu YH (2006) Influences of the crystallization behavior of n-HA reinforced PA66 biocomposite on its mechanical properties. Mater Sci Forum 510-511:898–901. https://doi.org/10.4028/www.scientific.net/MSF.510-511.898
25. Coniglio N, Sivarupan T, El Mansori M (2017) Investigation of process parameter effect on anisotropic properties of 3D printed sand molds. Int J Adv Manuf Technol 94(5–8):2175–2185. https://doi.org/10.1007/s00170-017-0861-5
26. Zhang Y, Zhang Y, Liu S, Huang A, Chi Z, Xu J, Economy J (2011) Phase stability and melting behavior of the α and γ phases of nylon 6. J Appl Polym Sci 120(4):1885–1891. https://doi.org/10.1002/app.33047